IEICE TRANS. FUNDAMENTALS, VOL. E81–A, NO. 4 APRIL 1998

PAPER

# Synchronization of Electric Fireflies by Using Square Wave Generators

**Takuji KOUSAKA**†, *Student Member*, **Hiroshi KAWAKAMI**†, *and* **Tetsushi UETA**†, *Members*

**SUMMARY** In this article, we propose a square wave generator whose switching threshold values are switched by external inputs. This circuit is designed to simulate the synchronized luminescence of coupled fireflies. We investigate the behavior of the solutions in two coupled oscillators. The dynamics are demonstrated by a linear autonomous equation piecewisely, therefore, a one-dimensional return map is derived. We also prove the existence of stable in-phase synchronization in the coupled oscillator by using the return map, and we show the existence of regions of periodic solutions within a parameter space. Some theoretical results are confirmed by laboratory measurements.

***key words:*** *square wave generator, piecewise linear system, synchronization, periodic solution, hysteresis*

## 1. Introduction

Cooperative behavior of living organisms can be regarded as one of nonlinear phenomena — synchronization of biological oscillations. As is well known, chirping crickets in the fields and luminescence of numerous fireflies around the riverside are typical biological synchronization in the natural world [1]. It is important to clarify these cooperative behavior in mathematical point of view.

We develop an electric firefly (abbr. EFF) by using a square wave generator. The EFF circuit has a photo-transistor and a photo-diode as input/output devices, so that a coupled EFF circuit is easily realized. Its dynamics is described by a simple mathematical model: four linear differential equations whose parameters are switched with threshold values. The system forms a switched dynamical system, thus behavior of the system looks like motion of billiard ball with moving rectangular borders.

There are some studies of similar switched dynamical systems. For example, Ref. [2] investigated neural type oscillator. He found out the existence of chaotic and fractal responses in the system by using an analytical method. In the following paper [3], Kohari et al. analyzed a hysteresis oscillator whose thresholds are varied periodically was investigated with a rigorous way. They showed a bifurcation diagram of the system and suggested the existence of a cantor-like set indicating hysteresis characteristics for some dominant periodic solutions.

Manuscript received September 8, 1997.
Manuscript revised November 20, 1997.

†The authors are with the Faculty of Engineering, Tokushima University, Tokushima-shi, 770–8506 Japan.

The coupld EFF circuits has more complicate conditions than the models treated above references. The switching conditions are different form. To analyze properties of the dynamics, we derive a one-dimensional return map explicitly. When two equivalent EFF circuits are coupled, there exists in-phase synchronization. We confirm the phenomenon with laboratory experiment and give a proof of the existence. When each EFF circuit has a different parameter, there exist various periodic solutions. We define the switching rate $\gamma$ by using input/output pulses and show a bifurcation diagram corresponding to some values of $\gamma$. The hysteresis characteristics are also found out.

## 2. Electric Fireflies

We develop an EFF circuit shown in Fig. 1. This is a simple square wave generator with a photo-diode and a photo-transistor. Note that the current does not flow into the photo-transistor when it is charged negative voltage.

If the photo-transistor is in OFF condition, then the circuit equation is described as

$$\begin{cases} R_2 C \dfrac{dv}{dt} + v = v_0, \\ v_+ = \dfrac{R_4}{R_3 + R_4} v_0 = \alpha v_0, \\ v_0 = E \ \mathrm{sgn}(v_+ - v) = E \ \mathrm{sgn}(\alpha v_0 - v). \end{cases} \tag{1}$$

By normalizing $v$ and $t$ as

$$\tau = \frac{1}{R_2 C} t, \quad x = \frac{v}{E}. \tag{2}$$

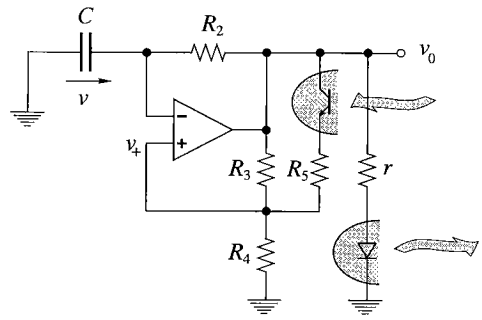


**Fig. 1** Electric firefly circuit (square wave generator).

Thus the first equation of Eqs. (1) becomes

$$\frac{dx}{d\tau} = -x \pm 1. \tag{3}$$

The period $\sigma$ of the square wave oscillation is given by:

$$\sigma_\alpha = 2\log\frac{1+\alpha}{1-\alpha}, \tag{4}$$

$$f_\alpha = \frac{1}{\sigma_\alpha}. \tag{5}$$

When photo-transistor is in ON condition, $v_+$ and period $\sigma_\beta$ are given by:

$$v_+ = \frac{R_3R_4 + R_4R_5}{R_3R_4 + R_3R_5 + R_4R_5}v_0 = \beta v_0 > \alpha v_0, \tag{6}$$

$$\sigma_\beta = 2\log\frac{1+\beta}{1-\beta}. \tag{7}$$

Hence we obtain the following relationship:

$$\sigma_\alpha - \sigma_\beta = 2\left(\log\frac{1+\alpha}{1-\alpha} - \log\frac{1+\beta}{1-\beta}\right) = 2\log\frac{(1+\alpha)(1-\beta)}{(1+\beta)(1-\alpha)} < 0. \tag{8}$$

This means that, when photo-transistor is in ON condition, the frequency is lower than the natural frequency Eq. (5) in OFF condition.

## 3. Coupled EFF Circuit

In the following we consider synchronization of a coupled EFF circuit shown in Fig. 2. The frequency of the output square wave can be controlled by the optical input signal of the other EFF circuit. The luminescene of the photo-diode can be considered as the fireflies' one.

We recast Eq. (3) as the following:

$$\frac{dv}{dt} = -v + e \ (e = -1 \text{ or } 1, \ v_+ = \pm\alpha \text{ or } \beta), \tag{9}$$

where $e$ denotes output voltage of the operational amplifier of an EFF circuit. Thus the equation of the coupled EFF circuit is described as:

$$\begin{cases} dv_1/dt = -v_1 + e_1 \\ \qquad (e_1 = -1 \text{ or } 1, \ v_{+1} = \pm\alpha_1 \text{ or } \beta_1) \\ dv_2/dt = -v_2 + e_2 \\ \qquad (e_2 = -1 \text{ or } 1, \ v_{+2} = \pm\alpha_2 \text{ or } \beta_2) \end{cases}, \tag{10}$$

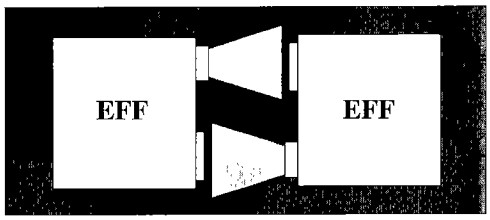


**Fig. 2** A coupled EFF circuit.

where $v_1$ and $v_2$ mean the voltage of the capacitor for each EFF circuit. From the previous section, Eq. (10) has the following relationship:

$$0 < \alpha_1 < \beta_1 < 1, \quad 0 < \alpha_2 < \beta_2 < 1. \tag{11}$$

Figure 3 shows an example of wave forms $v_i(t)$ and $e_i (i = 1, 2)$. However, in $v_1$-$v_2$ plane, a trajectory becomes a successive straight line because Eqs. (10) are independent and first-order linear differential equations, see Figs. 4, 5, 6 and 7.

We enumerate some properties for the coupled EFF circuit.

- The output voltage of the operational amplifier can be written by

$$e_i = \mathrm{sgn}(v_{+i} - v_i) \quad (i = 1, 2). \tag{12}$$

When $e_1$ and $e_2$ are equal to unity, both capacitor voltages of these circuits become unity. In this case, $v_{+i}$ switches from $\alpha_i$ to $\beta_i$ $(i = 1, 2)$. In the other cases $v_+$ stay $\alpha_i (i = 1, 2)$.

- When state becomes $v_1 = \beta_1$, $\alpha_2 \leqq v_2 \leqq \beta_2$ or $\alpha_1 \leqq v_1 \leqq \beta_1$, $v_2 = \beta_2$, the output switches from $(e_1, e_2) = (1, 1)$ to $(-1, -1)$.

For the following analysis we define some objects as follows:

$$P_1 \equiv \{(v_1, v_2) | -\alpha_1 \leqq v_1, v_2 \leqq \alpha_2, e_1 = -1, e_2 = 1\},$$

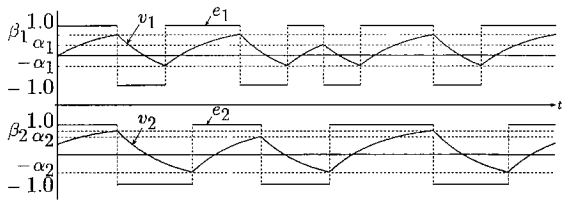


**Fig. 3** An example of wave form. $(\alpha_1 = 0.35, \alpha_2 = 0.6, \beta_1 = 0.7, \beta_2 = 0.8)$.

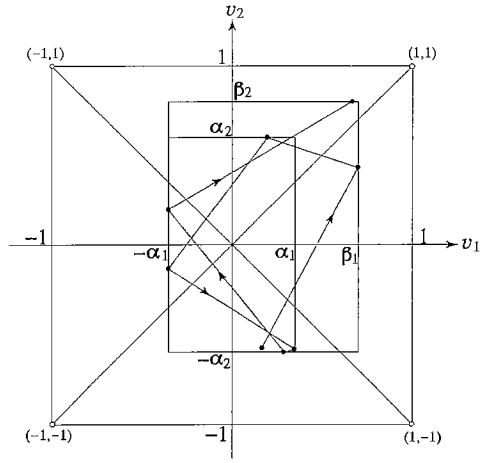


**Fig. 4** Phase portrait of an arbitrary trajectory in EFF circuits.

$$
\begin{aligned}
P_2 &\equiv \{(v_1,v_2)| -\alpha_1 \leqq v_1, -\alpha_2 \leqq v_2, e_1 = -1, \\
&\qquad e_2 = -1\}, \\
P_3 &\equiv \{(v_1,v_2)|v_1 \leqq \alpha_1, -\alpha_2 \leqq v_2, e_1 = 1, e_2 = -1\}, \\
P_4 &\equiv \{(v_1,v_2)|v_1 \leqq \beta_1, v_2 \leqq \beta_2, e_1 = 1, e_2 = 1\}.
\end{aligned} \tag{13}
$$

By using Eq. (13), Eq. (10) defines four linear differential equations on four half planes controlled by the optical input signal to the operational amplifier.

Note that the switch of the output of the operational amplifiers are owned by $v_i (i = 1, 2)$.

## 4. Return Map $F$

Since Eq. (10) is a piecewise linear autonomous system, we can calculate the solution of a coupled EFF circuit analytically, therefore, we can obtain a one-dimensional return map explicitly. The similar analysis technique is shown in Refs. [2], [3].

We define some intervals as follows:

$$
\begin{aligned}
I_{10} &\equiv \{(v_1,v_2)| -\alpha_1 \leqq v_1 \leqq \beta_1, v_2 = -\alpha_2, \\
&\qquad (v_1,v_2) \in P_1\}, \\
I_{20} &\equiv \{(v_1,v_2)|v_1 = \beta_1, -\alpha_2 < v_2 \leqq \beta_2, \\
&\qquad (v_1,v_2) \in P_1\}, \\
I_{30} &\equiv \{(v_1,v_2)| -\alpha_1 \leqq v_1 < \beta_1, v_2 = \beta_2, \\
&\qquad (v_1,v_2) \in P_3\}, \\
I_{40} &\equiv \{(v_1,v_2)|v_1 = -\alpha_1, -\alpha_2 < v_2 < \beta_2, \\
&\qquad (v_1,v_2) \in P_3\}, \\
I_{11} &\equiv \{(v_1,v_2)| -\alpha_1 \leqq v_1 \leqq \alpha_1, v_2 = -\alpha_2, \\
&\qquad (v_1,v_2) \in P_4\}, \\
I_{21} &\equiv \{(v_1,v_2)|v_1 = \alpha_1, -\alpha_2 < v_2 \leqq \beta_2, \\
&\qquad (v_1,v_2) \in P_2\}, \\
I_{31} &\equiv \{(v_1,v_2)| -\alpha_1 < v_1 \leqq \beta_1, v_2 = \alpha_2, \\
&\qquad (v_1,v_2) \in P_2\}, \\
I_{41} &\equiv \{(v_1,v_2)|v_1 = -\alpha_1, -\alpha_2 \leqq v_2 < \alpha_2, \\
&\qquad (v_1,v_2) \in P_4\}, \\
I_{51} &\equiv \{(v_1,v_2)|v_1 = \beta_1, \alpha_2 \leqq v_2 \leqq \beta_2, \\
&\qquad (v_1,v_2) \in P_2\}, \\
I_{61} &\equiv \{(v_1,v_2)|\alpha_1 \leqq v_1 \leqq \beta_1, v_2 = \beta_2, \\
&\qquad (v_1,v_2) \in P_2\}, \\
T_1 &= I_{10} \cup I_{20} \cup I_{30} \cup I_{40}, \\
T_2 &= I_{11} \cup I_{21} \cup I_{31} \cup I_{41} \cup I_{51} \cup I_{61}.
\end{aligned}
$$

Then any trajectory started from $T_1$ must jump onto $T_2$ and must return onto $T_1$. So we can define the following mapping:

$$
\begin{aligned}
f_1 &: T_1 \rightarrow T_2, \\
f_2 &: T_2 \rightarrow T_1, \\
f &: T_1 \rightarrow T_1, \quad f = f_2 \circ f_1.
\end{aligned} \tag{14}
$$

Also we define the following map.

$$
\begin{aligned}
\psi : T &\rightarrow S^1 \\
(v_1 \text{ or } v_2) &\rightarrow x
\end{aligned}, \tag{15}
$$

where, $S^1 = \{x \in \boldsymbol{R} \bmod 1\}$ and

$$
x = \begin{cases}
\dfrac{\alpha_1 + v_1}{2(\alpha_1 + \alpha_2 + \beta_1 + \beta_2)} & \text{for } v_1 \in I_{10} \\
\dfrac{\alpha_1 + \beta_1 + \alpha_2 + v_2}{2(\alpha_1 + \alpha_2 + \beta_1 + \beta_2)} & \text{for } v_2 \in I_{20} \\
\dfrac{\alpha_1 + \alpha_2 + 2\beta_1 + \beta_2 - v_1}{2(\alpha_1 + \alpha_2 + \beta_1 + \beta_2)} & \text{for } v_1 \in I_{30} \\
\dfrac{2(\alpha_1 + \beta_1 + \beta_2) + \alpha_2 - v_2}{2(\alpha_1 + \alpha_2 + \beta_1 + \beta_2)} & \text{for } v_2 \in I_{40}
\end{cases}. \tag{16}
$$

Finally we define the return map $F$ as:

$$
F \equiv \psi \circ f \circ \psi^{-1} \ : \ S^1 \rightarrow S^1. \tag{17}
$$

Consequently the dynamics of Eq. (10) can be interpreted as behavior of a discrete map written by:

$$
x_{n+1} = F(x_n). \tag{18}
$$

Figure 8 shows an examples of $F$ which corresponds to the parameters used in Fig. 3. In this figure $D_1$ and $D_2$ are:

$$
\begin{aligned}
D_1 &= \frac{\alpha_1 + \beta_1 + 2\alpha_2}{2(\alpha_1 + \alpha_2 + \beta_1 + \beta_2)}, \\
D_2 &= \frac{\alpha_2 + 2\beta_1 + \beta_2}{2(\alpha_1 + \alpha_2 + \beta_1 + \beta_2)},
\end{aligned} \tag{19}
$$

and $D_3$ and $D_4$ are assumed as:

- $D_3 \equiv$ A point on $I_{10} \cup I_{20}$ such that the trajectory started from $D_3$ hits $(v_1, v_2) = (-\alpha_1, \alpha_2)$
- $D_4 \equiv$ A point on $I_{30} \cup I_{40}$ such that the trajectory started from $D_4$ hits $(v_1, v_2) = (\alpha_1, -\alpha_2)$

Assume also that a point $x_p$ is called an $n$-periodic point of $F$ such that

$$
F^n(x_p) = x_p, F^k(x_p) \neq x_p \ (k < n). \tag{20}
$$

**Theorem 1:** $F$ has no fixed point.

**Proof:** Next two transitions have to be considered.

**case1**: $I_{10} \rightarrow I_{31} \rightarrow I_{10}$
**case2**: $I_{20} \rightarrow I_{41} \rightarrow I_{20}$
**case3**: $I_{30} \rightarrow I_{11} \rightarrow I_{30}$
**case4**: $I_{40} \rightarrow I_{21} \rightarrow I_{40}$

We show only case1. Let $x_0$ be an initial point on $I_{10}$. $x_0$ is transformed to a point $x_1 \in I_{31}$ and $x_1$ is transformed to a point $x_2 \in I_{10}$.

$$
x_2 = \frac{(\alpha_2 - 1)^2}{(\alpha_2 + 1)^2}(x_0 + 1) - 1. \tag{21}
$$

Here $x_2 < x_1 < x_0$. Hence $F$ has no fixed point. Analogous manner is possible for the other cases. □

## 5. Analysis

Firstly, two EFF circuits are connected each other and they have same parameters $(\alpha_1 = \alpha_2, \beta_1 = \beta_2)$.

**Theorem 2:** When two equivalent circuits are coupled, the rhythm of luminescence between EFF circuits synchronizes at in-phase.

**Proof:** We assume $\alpha = \alpha_1 = \alpha_2$, $\beta = \beta_1 = \beta_2$. When an initial point $x_a$ is located in $I_{10}$, it is possible below three cases for $F^2$ or $F^4$.

$$\begin{aligned}
\textbf{case1}\ (F^4): &\ x_a \in I_{10} \to x_b \in I_{41} \to x_c \in I_{30} \to \\
&\ x_d \in I_{61} \to x_e \in I_{40} \to x_f \in I_{11} \to \\
&\ x_g \in I_{20} \to x_h \in I_{51} \\
\textbf{case2}\ (F^4): &\ x_a \in I_{10} \to x_b \in I_{41} \to x_c \in I_{30} \to \\
&\ x_d \in I_{21} \to x_e \in I_{40} \to x_f \in I_{11} \to \\
&\ x_g \in I_{20} \to x_h \in I_{51} \\
\textbf{case3}\ (F^2): &\ x_a \in I_{10} \to x_b \in I_{41} \to x_c \in I_{30} \to \\
&\ x_d \in I_{21}
\end{aligned}$$

We show an explicit formulation in these cases.

**case1**:

$$g(v_1) = \frac{(\alpha-1)(\beta+1)(2(\alpha-1)-(\beta-1)(v_1+1))}{4(\alpha-1)-2(\beta-1)(v_1+1)+(\alpha-1)(\beta+1)(\beta-1)} - 1 \qquad (\alpha < v_1 < B_1),$$

**case2**:

$$g(v_1) = -\frac{(\alpha+1)(\alpha-1)(\beta+1)(v_1+1)}{2(\alpha+1)(v_1+1)-(\alpha-1)^2(\beta+1)} - 1 \qquad (B_1 < v_1 < B_2),$$

**case3**:

$$g(v_1) = \frac{(\alpha+1)(\beta-1)}{(\alpha-1)(\beta+1)}(v_1+1) - 1 \qquad (B_2 < v_1 < \alpha),$$

where,

$$B_1 = -\frac{(\alpha-1)^2}{\beta-1} - 1,$$

$$B_2 = -\frac{(\alpha-1)^2(\beta+1)}{(\alpha+1)(\beta-1)} - 1.$$

Hence we obtain the return map with $F^2$ and $F^4$.

$$G \equiv \psi \circ g \circ \psi^{-1} \ : \ S^1 \to S^1. \tag{22}$$

The difference equation on $S^1$ is given by replacing $F$ in Eq. (18) with $G$. In any cases, an initial point $x_0 \in I_{10}$ is larger than transformed the point $x_1 = G(x_0) \in I_{10}$. This means that any trajectory started from $x_0 \in I_{10}$ include case1. The stable fixed point of case1 has $x = 0$. $x = 0$ is equal to $(v_1, v_2) = (-\alpha, -\alpha)$. That is to say, the rhythm of luminescence between EFF circuits synchronizes at in-phase. □

In the following we analyze the coupled EFF circuit with different parameters $(\alpha_1 \neq \alpha_2, \beta_1 \neq \beta_2)$. Two EFFs synchronize at in-phase when they have same parameter $(\alpha_1 = \alpha_2)$. Figure 5 shows this trajectory. For characterize periodic trajectory, we show switching rate $\gamma$ as follows:

$$\gamma = \frac{\text{The number of } e_2 \text{ pulses}}{\text{The number of } e_1 \text{ pulses}} \quad \text{for } t \to \infty. \tag{23}$$

$\gamma$ corresponds to the next relation on one-dimensional return map.

$$\gamma = \frac{\text{The number of } x_{n+1} < x_n}{\text{The number of } x_{n+1} > x_n} \quad \text{for } t \to \infty. \tag{24}$$

Followings properties are known [4].

1. $\gamma$ exists and depends on the initial point $x$.
2. $\gamma$ is rational if $F$ has a stable periodic trajectory.

**Property:** If $\gamma = n/m$, the switch of output of the operational amplifier has $m+n$ switching. $F$ has $(m+n)/2$ periodic point and $m+n$ denotes the number of line segmentations of a trajectory on $v_1$-$v_2$ plane.

This means that $F$ is twice switching of output. For example, Fig. 9 shows phase portrait of 3 periodic point. This trajectory is symbolized by $\gamma = 4/2$ and the number of line segmentations is 6. Note that, when state becomes $v_1 = \beta_1$ and $\alpha_2 \leqq v_2 \leqq \beta_2$, the output switches from $(1, 1)$ to $(-1, -1)$.

Figure 10 shows the graph of the switching rate for $\alpha_2 = 0.7$, $\beta_1 = 0.7$, $\beta_2 = 0.8$. This figure means that Eq. (10) have many periodic trajectories. If $\alpha_2 < \alpha_1 < 1$, $\gamma$ is larger than 1, and if $\alpha_1 < \alpha_2 < 2$, $\gamma$ is smaller than 1. In some cases, if $\gamma$ is irrational, $F$ has an aperiodic trajectory.

Hereafter, we focus on the following range:

$$T_{3-i} > \log\frac{1+\alpha_{3-i}}{1-\alpha_{3-i}}, \quad \text{where } T_i = \log\frac{1+\beta_i}{1-\beta_i}\ (i = 1, 2). \tag{25}$$

When the output voltages of the operational amplifier $(v_{i0})$ are switched, we initialize $T_i = 0$. This means that $\gamma$ corresponds to $2/n$ or $n/2$. $F$ has stable $n+1$ periodic points and $2(n+1)$ denotes the number of line segmentations of a trajectory on $v_1$-$v_2$ plane.

Figure 11 shows $\gamma$ for various $\alpha_1$. We can see hysteresis characteristic and it is caused recursively.

We symbolize the periodic point by using the position of line segmentations of trajectory for obtaining more detailed information.

**Definition:**

$$\omega(v_1, v_2) = \begin{cases} 0 & \text{for } (v_1, v_2) \in I_{10} \text{ or } I_{11} \\ 1 & \text{for } (v_1, v_2) \in I_{20} \text{ or } I_{21} \\ 2 & \text{for } (v_1, v_2) \in I_{30} \text{ or } I_{31} \\ 3 & \text{for } (v_1, v_2) \in I_{40} \text{ or } I_{41} \end{cases}. \tag{26}$$

Under the condition Eq. (25), let us enumerate all possible cases for the solution of Eq. (10).

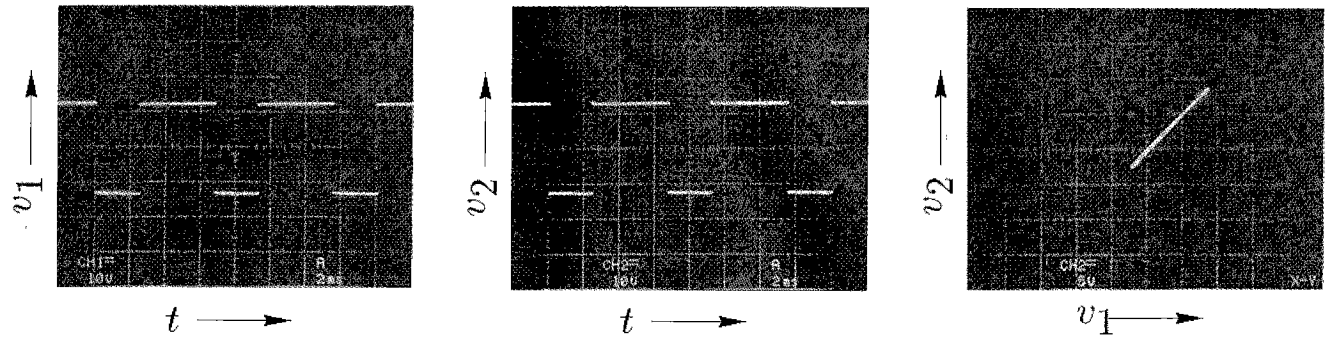


**Fig. 5** Laboratory measurement. $\alpha_1 \cong 0.2, \beta_1 \cong 0.7 (R_1 \cong 10\,\mathrm{k}\Omega, R_2 \cong 10\,\mathrm{k}\Omega, R_3 \cong 10\,\mathrm{k}\Omega, R_4 \cong 2.4\,\mathrm{k}\Omega, R_5 \cong 1.2\,\mathrm{k}\Omega, r \cong 100\,\Omega), \alpha_2 \cong 0.2, \beta_2 \cong 0.8 (R_1 \cong 10\,\mathrm{k}\Omega, R_2 \cong 10\,\mathrm{k}\Omega, R_3 \cong 10\,\mathrm{k}\Omega, R_4 \cong 2.4\,\mathrm{k}\Omega, R_5 \cong 680\,\Omega, r \cong 100\,\Omega)$, (waveforms: 2[ms/div], 10[v/div], phase portrait: 5[v/div], 5[v/div]).

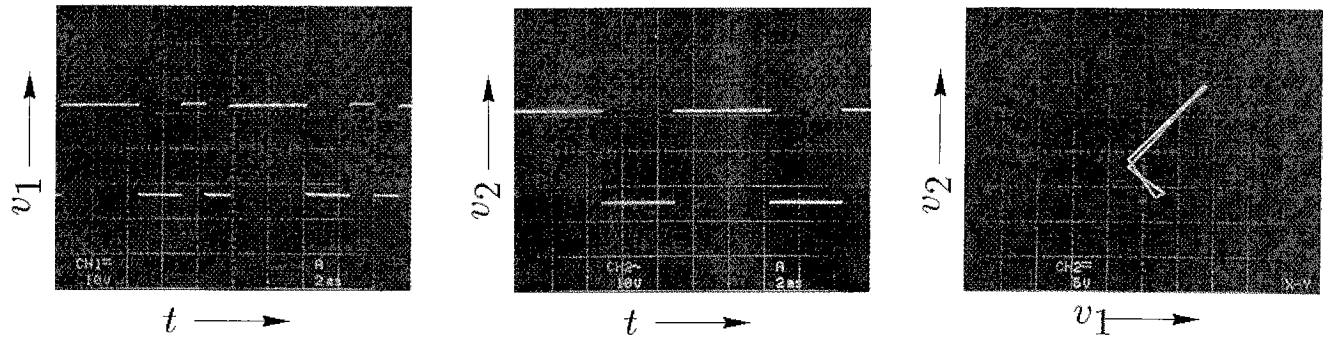


**Fig. 6** Laboratory measurement. $\alpha_1 \cong 0.2, \beta_1 \cong 0.7 (R_1 \cong 10\,\mathrm{k}\Omega, R_2 \cong 10\,\mathrm{k}\Omega, R_3 \cong 10\,\mathrm{k}\Omega, R_4 \cong 2.4\,\mathrm{k}\Omega, R_5 \cong 1.2\,\mathrm{k}\Omega, r \cong 100\,\Omega), \alpha_2 \cong 0.5, \beta_2 \cong 0.8 (R_1 \cong 10\,\mathrm{k}\Omega, R_2 \cong 10\,\mathrm{k}\Omega, R_3 \cong 10\,\mathrm{k}\Omega, R_4 \cong 10\,\mathrm{k}\Omega, R_5 \cong 3.3\,\mathrm{k}\Omega, r \cong 100\,\Omega)$.

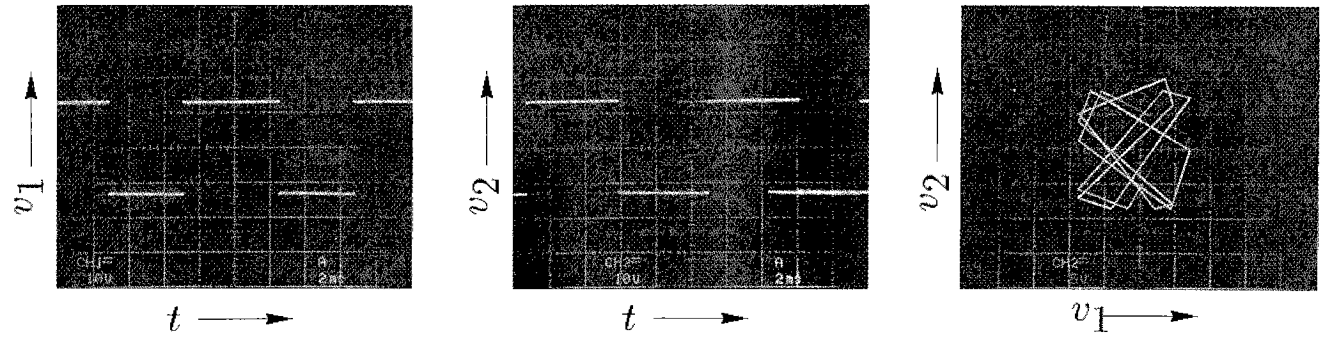


**Fig. 7** Laboratory measurement. $\alpha_1 \cong 0.5, \beta_1 \cong 0.7 (R_1 \cong 10\,\mathrm{k}\Omega, R_2 \cong 10\,\mathrm{k}\Omega, R_3 \cong 10\,\mathrm{k}\Omega, R_4 \cong 10\,\mathrm{k}\Omega, R_5 \cong 7.5\,\mathrm{k}\Omega, r \cong 100\,\Omega), \alpha_2 \cong 0.65, \beta_2 \cong 0.8 (R_1 \cong 10\,\mathrm{k}\Omega, R_2 \cong 10\,\mathrm{k}\Omega, R_3 \cong 10\,\mathrm{k}\Omega, R_4 \cong 18.4\,\mathrm{k}\Omega, R_5 \cong 9.1\,\mathrm{k}\Omega, r \cong 100\,\Omega)$.

$\gamma = 2/2n$ have $031(31)^{n-1}$, $301(31)^{n-1}$, $032(31)^{n-1}$, $302(31)^{n-1}$ and $\gamma = 2n/2$ have $(02)^{n-1}031$, $(02)^{n-1}301$, $(02)^{n-1}032$, $(02)^{n-1}302$, where a sequence (e.g. $031(31)^{n-1}$) means the order of $\omega(v_1, v_2)$ hit by a periodic trajectory. Figures 6, 9 and 12 show examples of wave form and phase portrait corresponds to 03131. This sequence 03131 is a kind of $\gamma = 4/2$.

The parameter regions of $\gamma = 2/(n-1)$ and $\gamma = 2/n$ are overlapped each other at any $n$. In such regions, some trajectories are coexist and they depend on the initial point. The regions $\gamma = (n-1)/2$ and $\gamma = n/2$ have similar structure. Figure 13 shows an example of return map for $\gamma = 2/2$ and $2/4$.

The stable fixed points disappear on $(v_1, v_2) = (\beta_1, \alpha_2)$ or $(\alpha_1, \beta_2)$. Figure 14 shows an example of return map and its wave form. This return map is constructed on $x$-$F^2(x)$ plane. When Fig. 14 (b) forms the boundary, it has totally different state between Figs. 14 (a) and (c). The output of the operational amplifier switches from $(e_1, e_2) = (1, 1)$ to

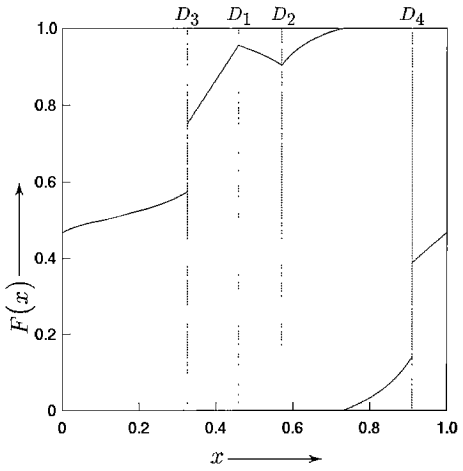


**Fig. 8** An example of return map.

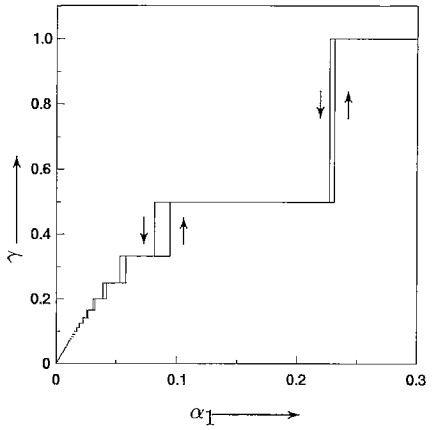


**Fig. 11** Hysteresis characteristic. ($\alpha_2 = 0.5$, $\beta_1 = 0.7$, $\beta_2 = 0.8$).

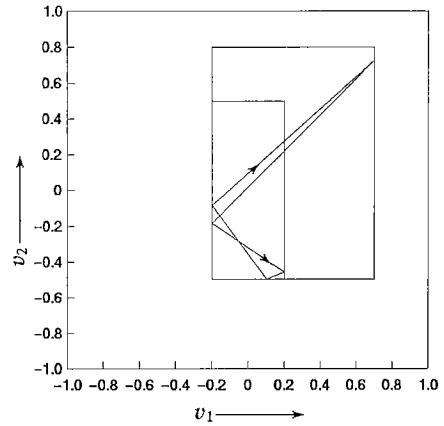


**Fig. 9** An example of phase space (03131). ($\alpha_1 = 0.2$, $\alpha_2 = 0.5$, $\beta_1 = 0.7$, $\beta_2 = 0.8$)

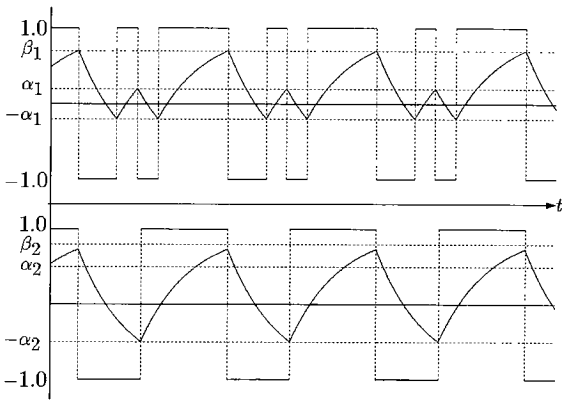


**Fig. 12** An example of wave form (03131). ($\alpha_1 = 0.2$, $\alpha_2 = 0.5, \beta_1 = 0.7, \beta_2 = 0.8$)

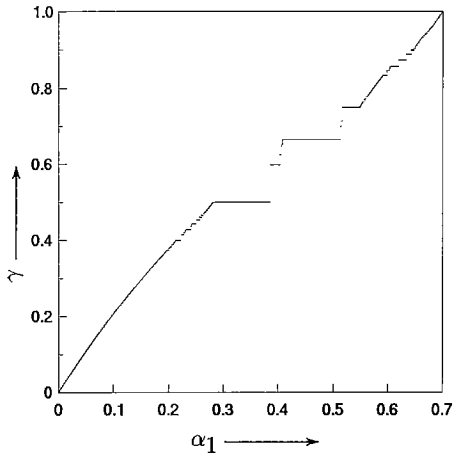


**Fig. 10** $\alpha_1$-$\gamma$ characteristic. $F^n(x)$, $n = 3000$, is used for the calculation of $\gamma$.

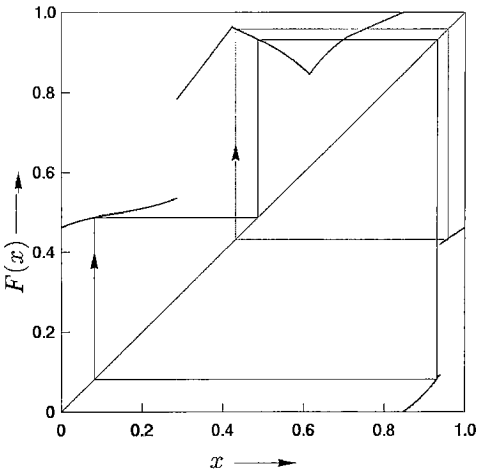


**Fig. 13** A Return map. There are two periodic trajectories corresponding to $\gamma = 2/2$ and $2/4$. $\alpha_1 = 0.2$, $\alpha_2 = 0.47$, $\beta_1 = 0.7$, $\beta_2 = 0.8$.

$(e_1, e_2) = (-1, -1)$ in Fig. 14(a). But in Fig. 14(c), the output of the operational amplifier switches from $(e_1, e_2) = (1, 1)$ to $(e_1, e_2) = (1, -1)$ or $(e_1, e_2) = (1, 1)$ to $(e_1, e_2) = (-1, 1)$. When parameter changes from Fig. 14(a) to Fig. 14(c), in general, the return map

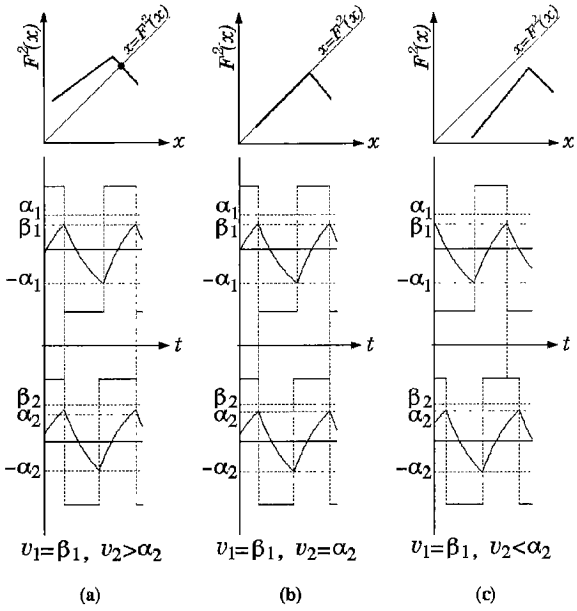


**Fig. 14** An example of return map and wave form near a singular bifurcation. This return map is constructed on $x$-$F^2(x)$ plane.

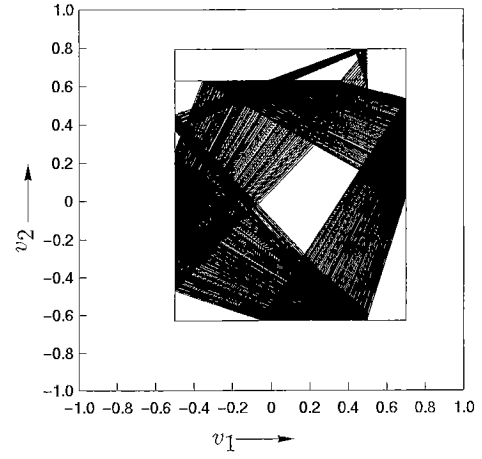


**Fig. 15** Asynchronous trajectory. ($\alpha_1 = 0.5$, $\alpha_2 = 0.63$, $\beta_1 = 0.7$, $\beta_2 = 0.8$)

forms the laminar phases. So a non-periodic trajectory like an intermittent solution is observed (See. Fig. 7, Fig. 15).

It is possible to derive existence region of these periodic trajectory. Figure 16 shows region of existence for several $\gamma$. $\gamma = 2/2$ have 013, 031, 032 and $\gamma = 2/4$ have 30131, 03231, 03131 in this parameter. When a denominator or a numerator of $\gamma$ is equal to 2, the trajectory never draw the double loop on a return map. In this case, showing the region of periodic trajectory is comparatively easy.

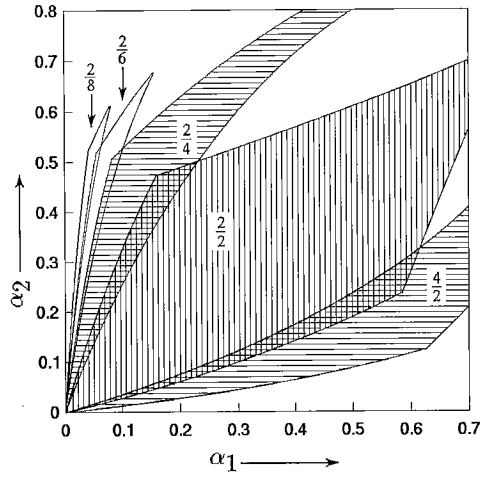


**Fig. 16** Bifurcation diagram. ($\beta_1 = 0.7$, $\beta_2 = 0.8$)

## 6. Conclusion

In this paper, we propose EFF circuit and analyze a coupled EFF circuit. They are described by piecewise linear autonomous equations, so that we derive one-dimensional return map explicitly. We prove the rhythm of luminescence between EFF circuits with same parameters synchronizes at in-phase. Also we show parameter regions for various kinds of periodic trajectories which includes hysteresis due to coexistence of trajectories. Some of theoretical results are confirmed by laboratory measurements.


### Acknowledgment

We would like to thank Prof. T. Saito, Hosei Univ., for his valuable comments and discussions on the basic matters of this work. We wish to thank Dr. K. Jin'no, Dr. K. Mitubori, Mr. H. Torikai, Mr. T. Tsubone and Mr. M. Wada for their helpful comments.


### References


[1] S.H. Strogatz and I. Stewart, "Synchronization of rhythm in creatures," SCIENTIFIC AMERICAN (Japanese edition) vol.269, no.11, pp.58–69, 1994.

[2] T. Saito and M. Oikawa, "Chaos and fractals from a forced artificial neural cell," IEEE Trans. on Neural Networks, vol.4, no.1, pp.43–52, 1993.

[3] K. Kohari, T. Saito, and H. Kawakami, "Chaos and hysteretic fractals from a hysteresis oscillator with periodic thresholds," Proc. NOLTA '92, pp.13–16, 1992.

[4] Y. Kaznelson, "Sigma-finite invariant measures from smooth mapping of the circle," J. D'Anal. Math., vol31, pp.744–750, 1988.

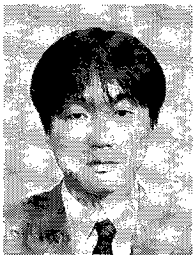

**Takuji Kousaka** received the B.E., M.E. from Tokushima University, Tokushima, Japan, in 1993 and 1995, respectively. His research interests are in bifurcation of discontinious nonlinear differential equations and its control.

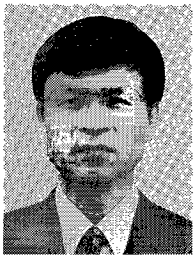

**Hiroshi Kawakami** received the B.E. degree from Tokushima University, Tokushima, Japan, in 1964, the M.E. and D.E. degrees from Kyoto University, Kyoto, Japan, in 1966 and 1974, respectively, all in electrical engineering. Presently, he is a professor of Electrical and Electronic Engineering, Tokushima University, Tokushima, Japan. His interest is qualitative properties of nonlinear circuits. kawakami@ee.tokushima-u.ac.jp

**Tetsushi Ueta** received the B.E., M.E., and D.E. from Tokushima University, Tokushima, Japan, in 1990, 1992 and 1996, respectively. He is an assistant professor of Information Science and Intelligent Systems, Tokushima University. His interests include bifurcation problems of dynamical systems and their visualization. tetsushi@is.tokushima-u.ac.jp, http://www-b1.is.tokushima-u.ac.jp/~tetsushi